

Surface analytical study of the interaction between γ -amino propyl triethoxysilane and E-glass surface

Part I *Time-of-flight secondary ion mass spectrometry*

D. WANG, F. R. JONES, P. DENISON

School of Materials, University of Sheffield, Mappin Street, Sheffield S1 3JD, UK

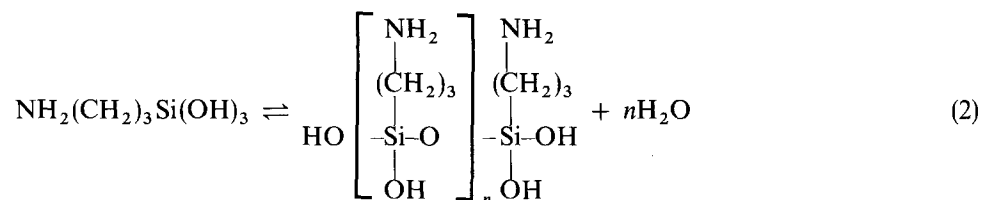
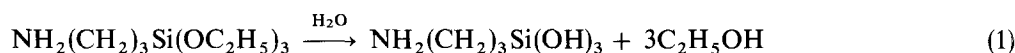
Time-of-flight secondary ion mass spectrometry has been used to study the interaction of γ -amino propyl triethoxysilane with an E-glass surface. The fragmentation pattern has been interpreted by assigning a series of mass peaks to the structural unit of the poly(aminosiloxane). The composition of the coating is complicated by the presence of polydimethylsiloxane and its copolymers. The highest mass fragment was obtained from the coating exposed by extraction with warm water (697 AMU). The largest molecular fragments would appear to have degrees of polymerization of 6 with differing numbers of silanol groups. On re-extraction with hot water the fragment size decreased. It is postulated that the network chain length of the three-dimensional polymer decreased as the interface was approached. At the glass surface a chemically bound molecular layer could be identified. The full chemical nature of the deposit is complicated by the incorporation of aluminium from the substrate into the coating. It was also possible to confirm that a layer of warm-water soluble oligomers existed at the air interface.

1. Introduction

Silane coupling agents are an important component of modern fibre-glass reinforced plastics enhancing the adhesion between glass fibre and matrix resin. γ -amino propyl triethoxysilane (APS) is widely used as a coupling agent for epoxy resins with which the amino group is believed to react. The APS is applied to the surface of freshly drawn glass fibres as a component of an aqueous size. APS, in the aqueous solution at a natural pH of 10.6, hydrolyses and rapidly condenses to give an equilibrium mixture of monomeric, oligomeric and polymeric siloxanols [1, 2]

the aminosilane deposit on a glass surface from aqueous solution consists of three distinct aminosilane layers [3, 9, 15, 16]. Adjacent to the glass surface, a few strongly chemisorbed molecular layers are formed, over which there is a weakly chemisorbed layer and at the outer surface a physisorbed layer. The two outer layers differ largely through their degrees of polymerization.

To date, this argument has been based on the variation in extraction rate under different aqueous conditions with some infrared back-up. In this paper we present direct evidence for the presence of a hetero-



The interaction between APS and glass surfaces has been extensively studied by X-ray photoelectron spectroscopy (XPS) [3-7], electron microscopy [8], ISS and secondary ion mass spectrometry (SIMS) [9], infrared spectroscopy [10-12] and nuclear magnetic resonance (NMR) [13, 14]. A consequence of the monomer-polymer equilibrium (Equation 2) is that

geneous deposit of differing molecular weight and cross-link density on the glass surface.

2. Experimental procedure

E-glass cullet, used in the fibre process, was cast into plates for cutting into slides of approximately 8 mm \times 8 mm \times 2 mm using a rotary diamond-impregnated

cutting wheel. These were ground to 1 mm thick, polished to better than 1 μm using a diamond paste polishing wheel, washed several times with deionized water, then heat cleaned at 200 °C for 0.5 h.

The slides were immersed into a 1.5 wt % solution of APS at natural pH (~ 10.6) in deionized water at room temperature for 45 min, then washed several times with deionized water (at room temperature) again and dried *in vacuo* at 50 °C. As a control, an as-polished plate was heat treated at 200 °C immediately prior to analysis. Some as-coated slides were conditioned in deionized water at 50 °C for 24 h, and some further conditioned at 100 °C for 4 h. The γ -amino propyl triethoxysilane (A1100) was supplied by Union Carbide.

The specimens were mounted on to a grid sample holder for analysis in a VG IX23S time-of-flight (TOF) SIMS instrument operating at a vacuum of $< 10^{-10}$ torr (1 torr = 133.322 Pa) with a micro-focused liquid Ga metal ion primary beam source (30 kV \times 1.0 nA). The spectra have been calibrated with well defined fragments in the low mass range from 0–300 AMU (e.g. Al^+ 27, PDMS(+)281). Without a fragment of known mass in the higher mass region, an assignment error of 1–2 AMU can arise. The figures in parentheses are the spectra mass numbers.

3. Results

3.1. Uncoated E-glass surface

3.1.1. Positive ions

The results, obtained from the untreated sample surface, show that TOF SIMS is really a sensitive technique for the analysis of glass surfaces, particularly for isotopic analysis. From Fig. 1a, we can see clearly two lithium isotopes at 6 and 7 AMU, two boron isotopes at 10 and 11 AMU, three magnesium isotopes at 24, 25 and 26 AMU, three silicon isotopes at 28, 29 and 30 AMU, four calcium isotopes at 40, 42, 43 and 44 AMU, and two copper isotopes at 63 and 65 AMU. The two gallium isotopes at 69 and 71 AMU result from the Ga ion primary beam used in the spectrometer. It is noted that the E-glass surface consists mainly of Si, Al and Ca. The fragments at 56 and 57 AMU represent CaO and CaOH.

3.1.2. Negative ions

The negative ion spectra (Fig. 1b) of the untreated sample show that oxygen and hydroxyl groups are the predominant species on the surface. The typical negative ion fragments, obtained from the glass surface, are SiO_2 , SiO_2H , SiO_3 and SiO_3H , as shown by mass peaks at 60, 61, 76 and 77 AMU, respectively. The mass fragments between 43 and 51 probably arise from hydrocarbon contaminants on the glass surface.

3.2. Coated E-glass surface

3.2.1. Positive ions

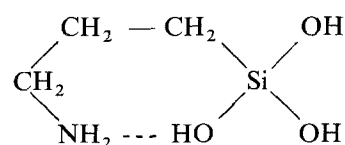
The positive ion spectra from the coated glass surface are shown in Fig. 2a. The peaks associated with Ca do not appear to be removed entirely; less intense peaks

at 40, 56 and 57 AMU remain. The APS treatment has led to a reduction in the intensities of these fragments rather than their removal. The other low mass fragment peaks are also of reduced intensity. The latter observation suggests that the aminosilane coating on the glass surface has a thickness less than the TOF SIMS sampling depth (~ 1 nm). But the XPS study (to be discussed elsewhere [17]) does demonstrate the absence of a Ca signal at a depth of about 3 nm for the warm-water extracted as-coated surface. Furthermore, the peaks at 40, 42, 43 and 44 AMU have not remained at the same ratio. Thus it is more likely that these small mass fragments arise from either the condensed $\text{Ca}(\text{OH})_2$ (CaOH –57 AMU) on the outermost layer or a component in the aminosilane coating which can be removed by warm-water extraction. Because, as shown in Table I, the mass fragments associated with Ca can be removed by warm-water washing, the former seems most probable. Therefore, it is concluded that a uniform silane coating has been deposited on to the glass surface. Thus the other secondary ion fragments desorbed from the coated slide must arise from the coating only. It also follows that because the intensity of the Al peak at 27 AMU was not affected by the silane treatment, Al has become an integral part of the surface coating. This conclusion was confirmed by analogous observations by XPS [17]. The following discussion is therefore based on the conclusion that the major components in the spectrum arise from the “silane” coating.

The peaks at 53, 55 and 57 AMU are typical of aliphatic hydrocarbons of the form $\text{C}_n\text{H}_{2n-3}$, $\text{C}_n\text{H}_{2n-1}$ and $\text{C}_n\text{H}_{2n+1}$.^{*} The peaks at 73, 147, 221; 133, 207, 281 are well documented as typical of polydimethyl siloxane (PDMS) [18]. Extensive studies to be reported elsewhere [17] have shown that there is a contaminant present in the original silane. These components give high ion yields and therefore are not directly indicative of a high concentration. A series of secondary ions analogous in structure to PDMS are also present for APS, whose structures are given in Table II.

On the basis of the equilibrium polymerization, as shown in Equation 2, we believe that the slightly less intense fragments at 119 and 120 AMU are typical of the fingerprint for the structural unit of the polymeric amino-siloxanols. The extended products of these fragments occur at 221 and 239 AMU, respectively. Their possible structures are also given in Table II, where it is seen that the peak at 221 AMU may arise from either component.

Koenig and co-workers [10, 11, 13] have demonstrated that the formation of an internally hydrogen-bonded cyclic structure



is responsible for the high concentration of monomers and oligomers in the equilibrium deposit on the glass

^{*} Note added in press. These have been shown to arise from contaminants since they are absent in spectra from fresh batches of APS.

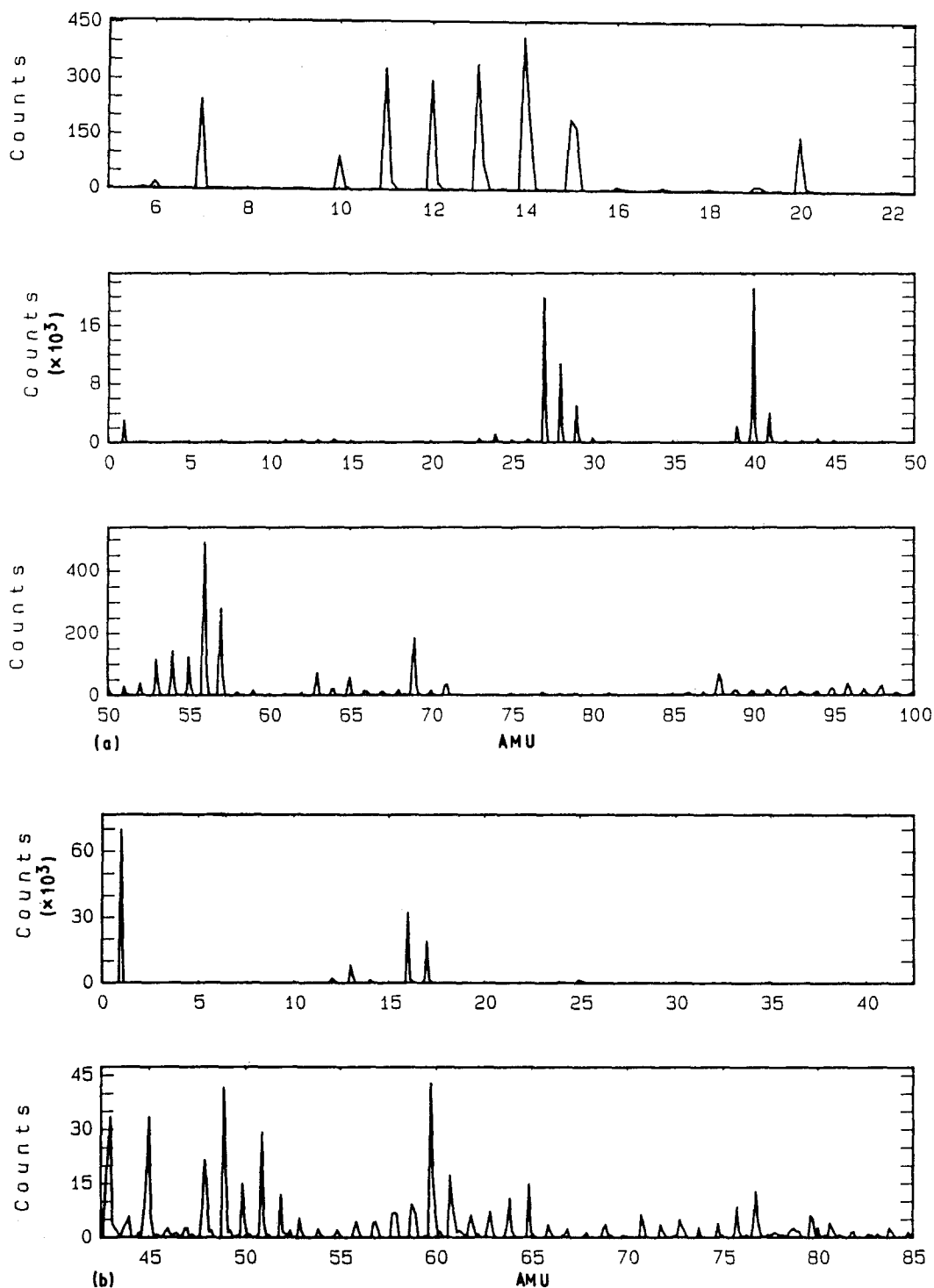


Figure 1 TOF SIMS spectra of (a) the positive ions and (b) the negative ions from the uncoated E-glass slides.

surface. It is not possible to differentiate between cyclic and linear secondary ion fragments nor between a cyclic or linear molecular source, however, the evidence in the literature would put high probability that the fragments at 119 and 120 AMU arise from the intramolecularly hydrogen-bonded monomers and oligomers present in the coating.

3.2.2. Negative ions

Regarding the negative ion spectra (Fig. 2b) of the coated surface, there are two fragments present at 75 and 77 AMU which probably arise from aluminium

oxide reaction products (see Table III). Two additional negative ion fragments which arise from the unhydrolysed aminosilane species appear at 127 and 128 AMU.

3.3. The as-coated glass surface after extraction with warm water

To confirm the presence of a layer of physisorbed oligomeric aminosilanes, the as-coated sample surface was immersed in warm water (50 °C) for 24 h. This is believed to remove the low molecular component without significant hydrolysis [16].

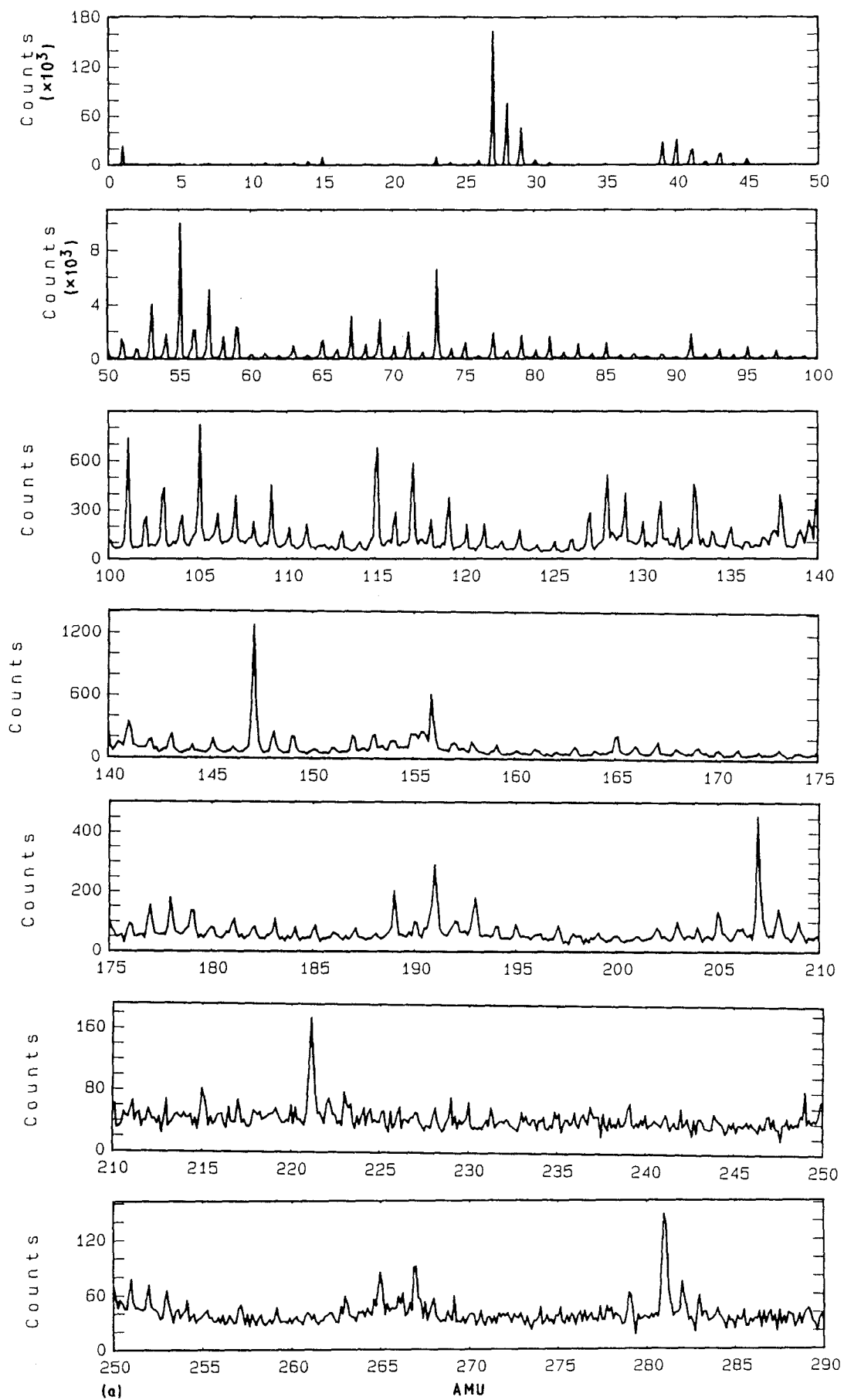


Figure 2 TOF SIMS spectra of (a) the positive ions and (b) the negative ions from the APS coated E-glass slides.

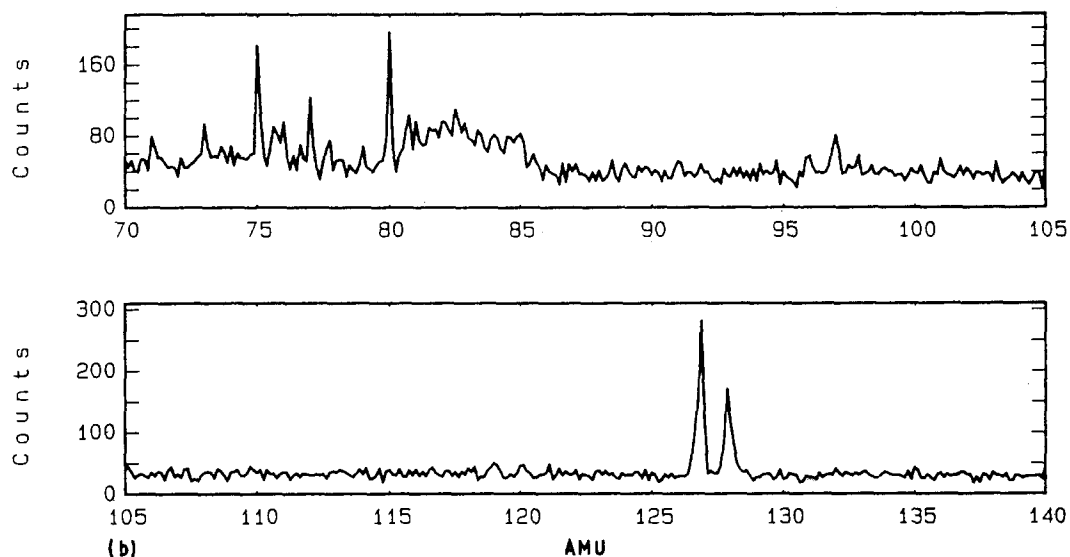


Figure 2 (b) (Contd.)

TABLE I The relative ratios of the positive ion peak intensities for Ca and Al species

Surface	Ca/Al	CaO/Al	CaOH/Al	Total
Uncoated	1.07	0.03	0.01	1.10
Coated	0.19	0.01	0.03	0.23
Warm-water extracted	0.00	0.00	0.00	0.00
Hot-water extracted	0.38	0.08	0.30	0.76

3.3.1. Positive ions

From Fig. 3a it can be seen that the extraction resulted in the emergence of a series of relatively high mass ion fragments from 340–697(695) AMU, compared to the as-coated sample which exhibited the largest APS mass of fragment at 221 AMU. This confirms that a higher molecular weight layer has been exposed by the warm-water extraction and that the readily extractable physisorbed component is essentially oligomeric. The molecular size of the more highly resistant component appears to be at least two and a half times larger than those in the physisorbed layer in terms of the ratio of molecular weight of the largest fragments at 697(695) and 221 AMU of ≈ 3.2 .

The possible structures for these fragments of 340–697(695) AMU are shown in Table IV. The seven fragments at 358, 477, 596; 340, 459, 578 and 697(695) AMU consist of linear and cyclic oligomers with the largest containing six repeat units. An analogous series of PDMS fragments and copolymers of APS and PDMS are also observed. Accordingly, these oligomers or polymers probably represent the principal composition just below the physisorbed layer. These arise from fragmentation of a more highly polymerized structure.

3.3.2. Negative ions

The deposit remaining after extraction also gave a series of relatively high mass negative ion fragments

from 91–322 AMU (see Fig. 3b). Possible structures are presented in Table V. Prior to warm-water conditioning, the highest mass fragment occurred at 128 AMU. Clearly, the molecular weight ratio for 322 and 128 AMU is ≈ 2.5 , confirming the presence of a coating with a significantly higher degree of polymerization. As will be discussed below, this is better understood in terms of a highly cross-linked polymer because the fragmentation is more complicated than that expected of a linear polymer.

3.4. The warm-water conditioned as-coated glass surface after extraction with hot water

In order to identify whether a chemisorbed layer was present at the silane-glass interface, the warm-water conditioned coated glass slides were subsequently extracted with hot water (100°C) for 4 h.

3.4.1. Positive ions

Fig. 4a shows that after further extraction with hot water all of the relatively high mass fragments from 416–697(695) AMU were absent with the largest mass fragment at 358 AMU. The possible structures for the fragments from this conditioned surface are shown in Table VI. The 358 AMU fragment consists of three linear units only. This could arise from a network end whereas the cyclic fragment at 340 AMU might come from the network polymer. The reduction in the molecular size of the largest secondary ion is consistent with the exposure of an insoluble molecular layer which is either strongly adsorbed to the immediate glass surface or consists of a cross-linked polymer. Because the former situation also results in a high cross-link density it follows that the small fragment size reflects the average network chain length.

3.4.2. Negative ions

The negative ion spectra from this reconditioned sample are shown in Fig. 4b. There are present five

TABLE II Possible structures for positive ion fragments from the coated glass slides

AMU	Fragment	AMU	Fragment
73	$\text{CH}_3-\text{Si}\left(\begin{array}{c} \text{CH}_3 \\ \\ \text{CH}_3 \end{array}\right)-\text{O}-\text{Si}^+\left(\begin{array}{c} \text{CH}_3 \\ \\ \text{CH}_3 \end{array}\right)_0$	119	$\begin{array}{c} \text{NH}_2 \\ \\ (\text{CH}_2)_3 \\ \\ \text{O}-\text{Si}^+ \\ \\ \text{OH} \end{array}$
147	$\text{CH}_3-\text{Si}\left(\begin{array}{c} \text{CH}_3 \\ \\ \text{CH}_3 \end{array}\right)-\text{O}-\text{Si}^+\left(\begin{array}{c} \text{CH}_3 \\ \\ \text{CH}_3 \end{array}\right)_1$	120	$\text{HO}-\text{Si}\left(\begin{array}{c} \text{NH}_2 \\ \\ (\text{CH}_2)_3 \\ \\ \text{OH} \end{array}\right)-\text{O}-\text{Si}^+\left(\begin{array}{c} \text{NH}_2 \\ \\ (\text{CH}_2)_3 \\ \\ \text{OH} \end{array}\right)_0$
221	$\text{CH}_3-\text{Si}\left(\begin{array}{c} \text{CH}_3 \\ \\ \text{CH}_3 \end{array}\right)-\text{O}-\text{Si}^+\left(\begin{array}{c} \text{CH}_3 \\ \\ \text{CH}_3 \end{array}\right)_2$	239	$\text{HO}-\text{Si}\left(\begin{array}{c} \text{NH}_2 \\ \\ (\text{CH}_2)_3 \\ \\ \text{OH} \end{array}\right)-\text{O}-\text{Si}^+\left(\begin{array}{c} \text{NH}_2 \\ \\ (\text{CH}_2)_3 \\ \\ \text{OH} \end{array}\right)_1$
133	$\begin{array}{c} \text{CH}_3 \\ \\ \text{Si}^+ \\ / \quad \backslash \\ \text{O} \quad \text{O} \\ / \quad \backslash \quad / \quad \backslash \\ \text{Si} \quad \text{Si} \\ / \quad \backslash \quad / \quad \backslash \\ \text{CH}_3 \quad \text{O} \quad \text{CH}_3 \end{array} \left[\begin{array}{c} \text{CH}_3 \\ \\ \text{O} \\ / \quad \backslash \\ \text{Si} \quad \text{Si} \\ / \quad \backslash \quad / \quad \backslash \\ \text{CH}_3 \quad \text{O} \quad \text{CH}_3 \end{array} \right]_0$	221	$\begin{array}{c} \text{NH}_2 \\ \\ (\text{CH}_2)_3 \\ \\ \text{Si}^+ \\ / \quad \backslash \\ \text{HO} \quad \text{O} \\ / \quad \backslash \quad / \quad \backslash \\ \text{Si} \quad \text{Si} \\ / \quad \backslash \quad / \quad \backslash \\ (\text{CH}_2)_3 \quad \text{O} \quad (\text{CH}_2)_3 \\ \quad \quad \quad \\ \text{NH}_2 \quad \quad \quad \text{NH}_2 \end{array} \left[\begin{array}{c} \text{NH}_2 \\ \\ (\text{CH}_2)_3 \\ \\ \text{O} \\ / \quad \backslash \\ \text{Si} \quad \text{Si} \\ / \quad \backslash \quad / \quad \backslash \\ (\text{CH}_2)_3 \quad \text{O} \quad (\text{CH}_2)_3 \\ \quad \quad \quad \\ \text{NH}_2 \quad \quad \quad \text{NH}_2 \end{array} \right]_0$
207	$\begin{array}{c} \text{CH}_3 \\ \\ \text{Si}^+ \\ / \quad \backslash \\ \text{O} \quad \text{O} \\ / \quad \backslash \quad / \quad \backslash \\ \text{Si} \quad \text{Si} \\ / \quad \backslash \quad / \quad \backslash \\ \text{CH}_3 \quad \text{O} \quad \text{CH}_3 \end{array} \left[\begin{array}{c} \text{CH}_3 \\ \\ \text{O} \\ / \quad \backslash \\ \text{Si} \quad \text{Si} \\ / \quad \backslash \quad / \quad \backslash \\ \text{CH}_3 \quad \text{O} \quad \text{CH}_3 \end{array} \right]_1$		
281	$\begin{array}{c} \text{CH}_3 \\ \\ \text{Si}^+ \\ / \quad \backslash \\ \text{O} \quad \text{O} \\ / \quad \backslash \quad / \quad \backslash \\ \text{Si} \quad \text{Si} \\ / \quad \backslash \quad / \quad \backslash \\ \text{CH}_3 \quad \text{O} \quad \text{CH}_3 \end{array} \left[\begin{array}{c} \text{CH}_3 \\ \\ \text{O} \\ / \quad \backslash \\ \text{Si} \quad \text{Si} \\ / \quad \backslash \quad / \quad \backslash \\ \text{CH}_3 \quad \text{O} \quad \text{CH}_3 \end{array} \right]_2$		

TABLE III Possible structures for negative ion fragments from the coated glass slides

AMU	Fragment	AMU	Fragment
75	$\text{AlO}_3^-/\text{CH}_3\text{SiO}_2^-$	77	AlO_3H_2^-
80	$\text{C}_5\text{H}_6\text{N}^-$	127	$\text{CH}_2=\text{CH}-\text{CH}=\text{CH}-\text{Si}(\text{CH}_3)_2\text{O}^-$
128	$\text{NH}=\text{CH}-\text{CH}=\text{CH}-\text{Si}(\text{CH}_3)_2\text{O}^-$		

peaks at 149(147), 163, 237; 221 and 255(253) AMU, respectively, and their possible structures are given in Table VII. The largest fragment, 255(253) AMU, is a dimer confirming that the interfacial layer has a high cross-link density.

4. Discussion

The deposition of an aminosilane from aqueous solution at natural pH, has been found to have layers of differing hydrolytic stabilities in confirmation of the work of Koenig and co-workers [10-13] and Schrader

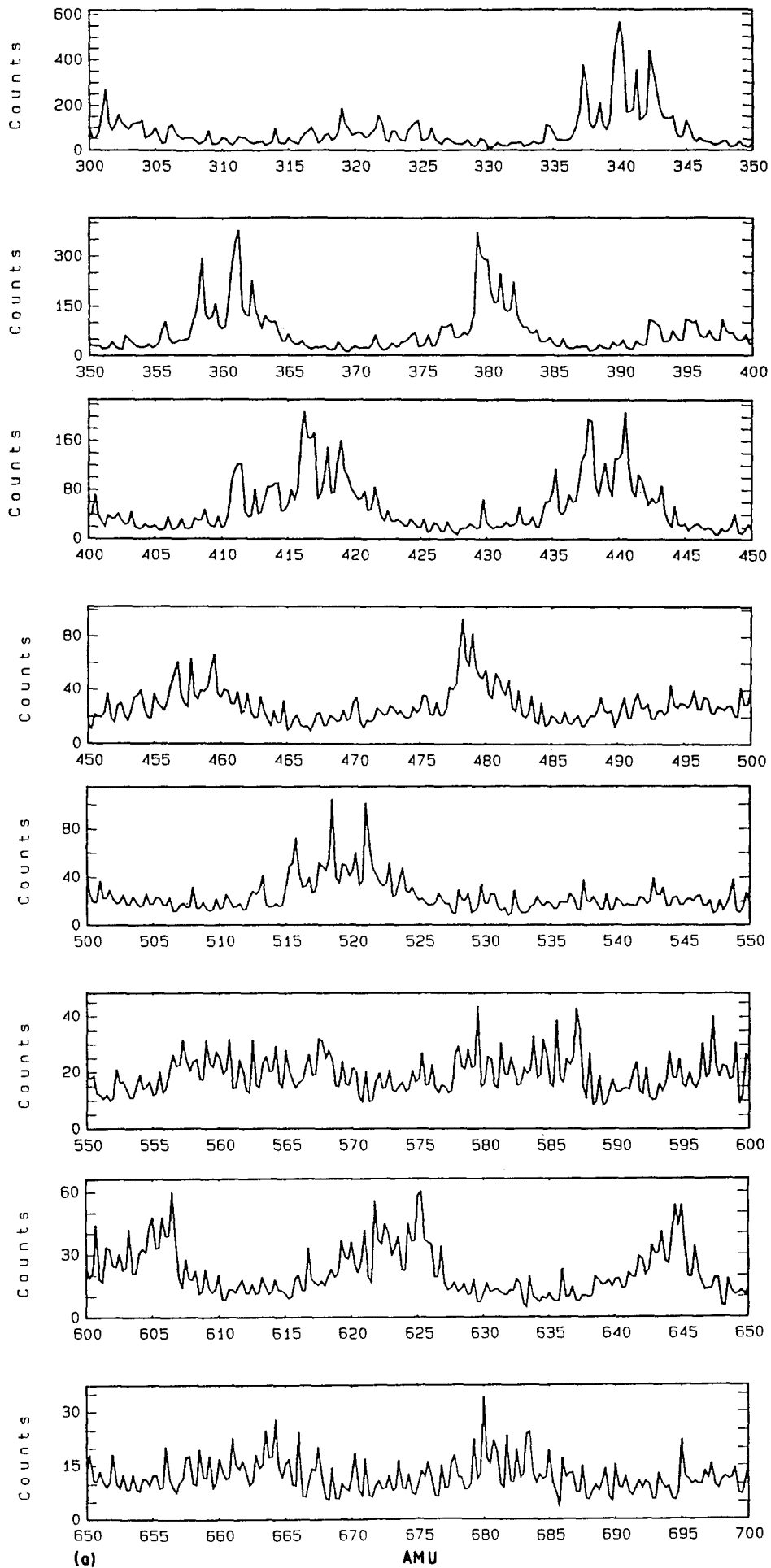


Figure 3 TOF SIMS spectra of (a) the positive ions and (b) the negative ions from the warm-water conditioned as-coated glass slides.

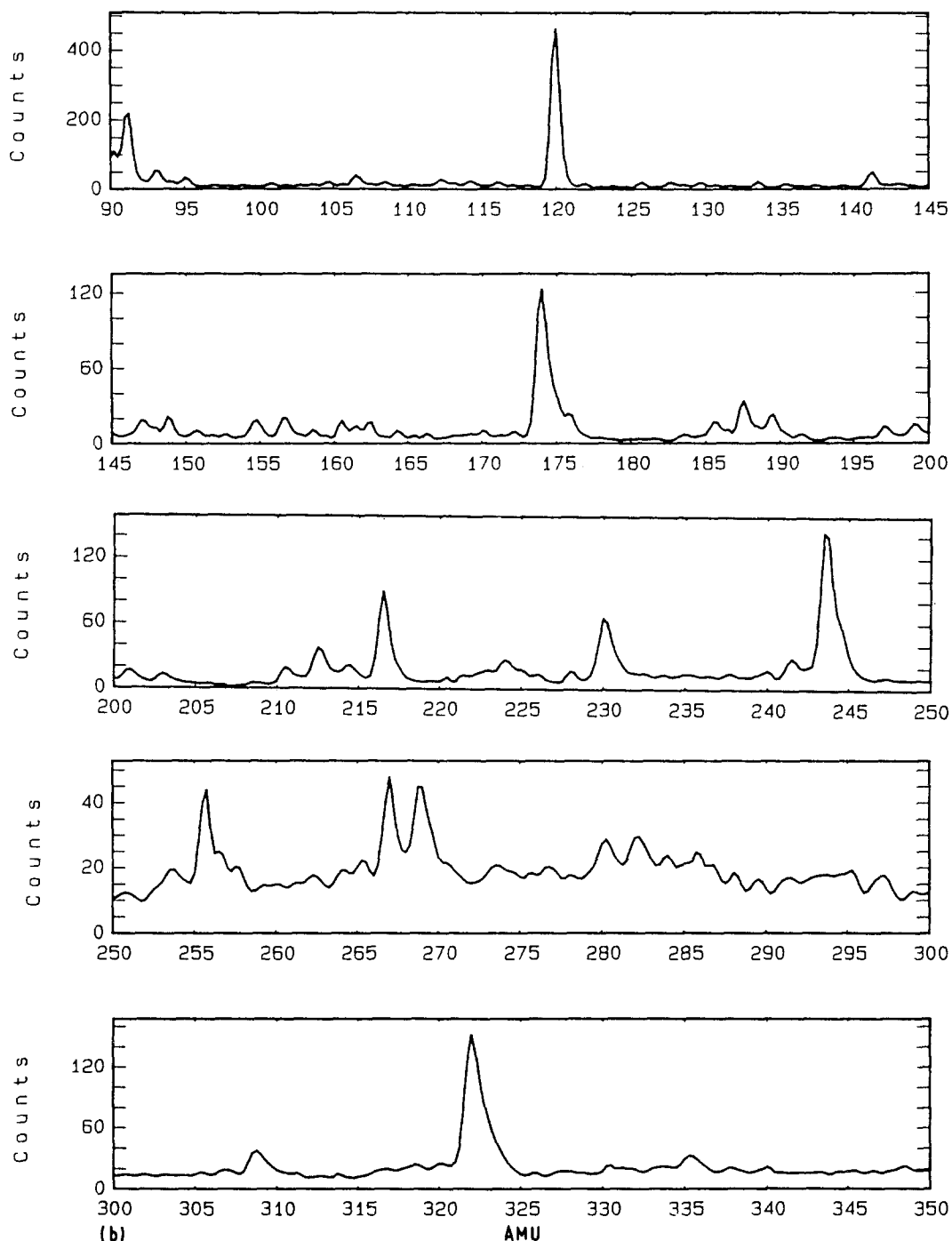


Figure 3 (b) (Contd.)

et al. [16] In order to examine the molecular structure of these components, standard extraction procedures have been used to expose the differing layers: physisorbed, three-dimensional (or cross-linked) and interfacial layers.

4.1. Physisorbed layer

In the XPS studies [17] it was shown that the APS coating on the coated glass surface is at least about 3 nm thick. Since with TOF SIMS we are examining the outer molecular layers of the coating, the interpretation of the TOF SIMS analysis applies to the outer layer of the aminosilane coating. TOF SIMS imaging [18] has also confirmed that APS is uniformly coated on to analogous E-glass fibres. At the air interface a physisorbed layer is present which can be removed by immersion in warm water and which

mainly consists of small molecular oligomers (see Table II) as demonstrated by a mass fragmentation pattern which is dominated by PDMS and APS linear units.

The largest fragment sputtered from the as-coated glass surface occurs at 281 AMU which is much larger than the mass fragment at 73 AMU reported for *N,N*-dimethyl aminotrimethylsilane modified boron silicate glass surface by Lub *et al.* [19] also using TOF SIMS.

These results confirm the arguments of Koenig and co-workers [10–13] who reported that the physisorbed outer layer mainly consisted of small oligomers.

4.2. Three-dimensional (or cross-linked) layer

From this layer some APS fragments containing five or six structural units were observed, such as 596, 578

TABLE IV Possible structures for positive ion fragments from the warm-water conditioned as-coated glass slides (The mass number in parentheses refers to the observed fragment in the spectrum.)

AMU	Fragment	AMU	Fragment
443 (441)	$\text{CH}_3-\text{Si}\left(\begin{array}{c} \text{CH}_3 \\ \\ \text{CH}_3 \end{array}\right)-\text{O}-\text{Si}^+\left(\begin{array}{c} \text{CH}_3 \\ \\ \text{CH}_3 \end{array}\right)_5$	358	$\text{HO}-\text{Si}\left(\begin{array}{c} \text{NH}_2 \\ \\ (\text{CH}_2)_3 \\ \\ \text{OH} \end{array}\right)-\text{O}-\text{Si}^+\left(\begin{array}{c} \text{NH}_2 \\ \\ (\text{CH}_2)_3 \\ \\ \text{OH} \end{array}\right)_2$
517	$\text{CH}_3-\text{Si}\left(\begin{array}{c} \text{CH}_3 \\ \\ \text{CH}_3 \end{array}\right)-\text{O}-\text{Si}^+\left(\begin{array}{c} \text{CH}_3 \\ \\ \text{CH}_3 \end{array}\right)_6$	477	$\text{HO}-\text{Si}\left(\begin{array}{c} \text{NH}_2 \\ \\ (\text{CH}_2)_3 \\ \\ \text{OH} \end{array}\right)-\text{O}-\text{Si}^+\left(\begin{array}{c} \text{NH}_2 \\ \\ (\text{CH}_2)_3 \\ \\ \text{OH} \end{array}\right)_3$
605	$\text{CH}_3-\text{Si}\left(\begin{array}{c} \text{CH}_3 \\ \\ \text{CH}_3 \end{array}\right)-\text{O}-\text{Si}^+\left(\begin{array}{c} \text{CH}_3 \\ \\ \text{CH}_3 \end{array}\right)-\text{CH}_2^+$	596	$\text{HO}-\text{Si}\left(\begin{array}{c} \text{NH}_2 \\ \\ (\text{CH}_2)_3 \\ \\ \text{OH} \end{array}\right)-\text{O}-\text{Si}^+\left(\begin{array}{c} \text{NH}_2 \\ \\ (\text{CH}_2)_3 \\ \\ \text{OH} \end{array}\right)_4$
355	$\left[\begin{array}{c} \text{CH}_3 \\ \\ \text{Si}^+ \\ / \quad \backslash \\ \text{O} \quad \text{O} \\ / \quad \backslash \\ \text{Si} \quad \text{Si} \\ / \quad \backslash \\ \text{CH}_3 \quad \text{CH}_3 \\ \quad \\ \text{CH}_3 \quad \text{CH}_3 \end{array} \right]_3$	340	$\left[\begin{array}{c} \text{NH}_2 \\ \\ (\text{CH}_2)_3 \\ \\ \text{Si}^+ \\ / \quad \backslash \\ \text{HO} \quad \text{O} \quad \text{O} \quad \text{OH} \\ / \quad \backslash \\ \text{Si} \quad \text{Si} \\ / \quad \backslash \\ (\text{CH}_2)_3 \quad \text{O} \quad (\text{CH}_2)_3 \\ \quad \\ \text{NH}_2 \quad \text{NH}_2 \end{array} \right]_1$
429	$\left[\begin{array}{c} \text{CH}_3 \\ \\ \text{Si}^+ \\ / \quad \backslash \\ \text{O} \quad \text{O} \\ / \quad \backslash \\ \text{Si} \quad \text{Si} \\ / \quad \backslash \\ \text{CH}_3 \quad \text{CH}_3 \\ \quad \\ \text{CH}_3 \quad \text{CH}_3 \end{array} \right]_4$	459	$\left[\begin{array}{c} \text{NH}_2 \\ \\ (\text{CH}_2)_3 \\ \\ \text{Si}^+ \\ / \quad \backslash \\ \text{HO} \quad \text{O} \quad \text{O} \quad \text{OH} \\ / \quad \backslash \\ \text{Si} \quad \text{Si} \\ / \quad \backslash \\ (\text{CH}_2)_3 \quad \text{O} \quad (\text{CH}_2)_3 \\ \quad \\ \text{NH}_2 \quad \text{NH}_2 \end{array} \right]_2$
383	$\text{CH}_3-\text{Si}\left(\begin{array}{c} \text{CH}_3 \\ \\ \text{CH}_3 \end{array}\right)-\text{O}-\text{Si}\left(\begin{array}{c} \text{CH}_3 \\ \\ \text{CH}_3 \end{array}\right)-\left[\text{O}-\text{Si}^+\left(\begin{array}{c} \text{NH}_2 \\ \\ (\text{CH}_2)_3 \\ \\ \text{OH} \end{array}\right) \right]_2$	578	$\left[\begin{array}{c} \text{NH}_2 \\ \\ (\text{CH}_2)_3 \\ \\ \text{Si}^+ \\ / \quad \backslash \\ \text{HO} \quad \text{O} \quad \text{O} \quad \text{OH} \\ / \quad \backslash \\ \text{Si} \quad \text{Si} \\ / \quad \backslash \\ (\text{CH}_2)_3 \quad \text{O} \quad (\text{CH}_2)_3 \\ \quad \\ \text{NH}_2 \quad \text{NH}_2 \end{array} \right]_3$
681	$\text{CH}_3-\text{Si}\left(\begin{array}{c} \text{CH}_3 \\ \\ \text{CH}_3 \end{array}\right)-\text{O}-\text{Si}\left(\begin{array}{c} \text{CH}_3 \\ \\ \text{CH}_3 \end{array}\right)-\left[\text{O}-\text{Si}^+\left(\begin{array}{c} \text{NH}_2 \\ \\ (\text{CH}_2)_3 \\ \\ \text{OH} \end{array}\right) \right]_5$	697 (695)	$\left[\begin{array}{c} \text{NH}_2 \\ \\ (\text{CH}_2)_3 \\ \\ \text{Si}^+ \\ / \quad \backslash \\ \text{HO} \quad \text{O} \quad \text{O} \quad \text{OH} \\ / \quad \backslash \\ \text{Si} \quad \text{Si} \\ / \quad \backslash \\ (\text{CH}_2)_3 \quad \text{O} \quad (\text{CH}_2)_3 \\ \quad \\ \text{NH}_2 \quad \text{NH}_2 \end{array} \right]_4$

TABLE VI Possible structures for positive ion fragments from the hot-water conditioned as-coated glass slides (The mass number in parentheses refers to the observed fragment in the spectrum.)

AMU	Fragment	AMU	Fragment
358 (356)	$\begin{array}{c} \text{NH}_2 \\ \\ (\text{CH}_2)_3 \\ \\ \text{HO}-\text{Si}- \\ \\ \text{OH} \end{array} \left[\begin{array}{c} \text{NH}_2 \\ \\ (\text{CH}_2)_3 \\ \\ \text{O}-\text{Si}^+ \\ \\ \text{OH} \end{array} \right]_2$	340	$\begin{array}{c} \text{NH}_2 \\ \\ (\text{CH}_2)_3 \\ \\ \text{Si}^+ \\ / \quad \backslash \\ \text{HO} \quad \text{O} \quad \text{O} \quad \text{OH} \\ \quad \quad \\ \text{Si} \quad \text{Si} \\ / \quad \backslash \quad / \quad \backslash \\ (\text{CH}_2)_3 \quad \text{O} \quad (\text{CH}_2)_3 \\ \quad \quad \quad \\ \text{NH}_2 \quad \quad \quad \text{NH}_2 \end{array} \left. \vphantom{\begin{array}{c} \text{NH}_2 \\ \\ (\text{CH}_2)_3 \\ \\ \text{Si}^+ \\ / \quad \backslash \\ \text{HO} \quad \text{O} \quad \text{O} \quad \text{OH} \\ \quad \quad \\ \text{Si} \quad \text{Si} \\ / \quad \backslash \quad / \quad \backslash \\ (\text{CH}_2)_3 \quad \text{O} \quad (\text{CH}_2)_3 \\ \quad \quad \quad \\ \text{NH}_2 \quad \quad \quad \text{NH}_2 \end{array}} \right]_1$
327 (325)	$\begin{array}{c} \text{NH}_2 \\ \\ (\text{CH}_2)_3 \\ \\ \text{HO}-\text{Si}- \\ \\ \text{OH} \end{array} - \text{O} - \begin{array}{c} \text{NH}_2 \\ \\ (\text{CH}_2)_3 \\ \\ \text{Si} \\ \\ \text{OH} \end{array} - \text{O} - \begin{array}{c} \text{CH}_3 \\ \\ \text{Si}-\text{CH}_2^+ \\ \\ \text{CH}_3 \end{array}$		

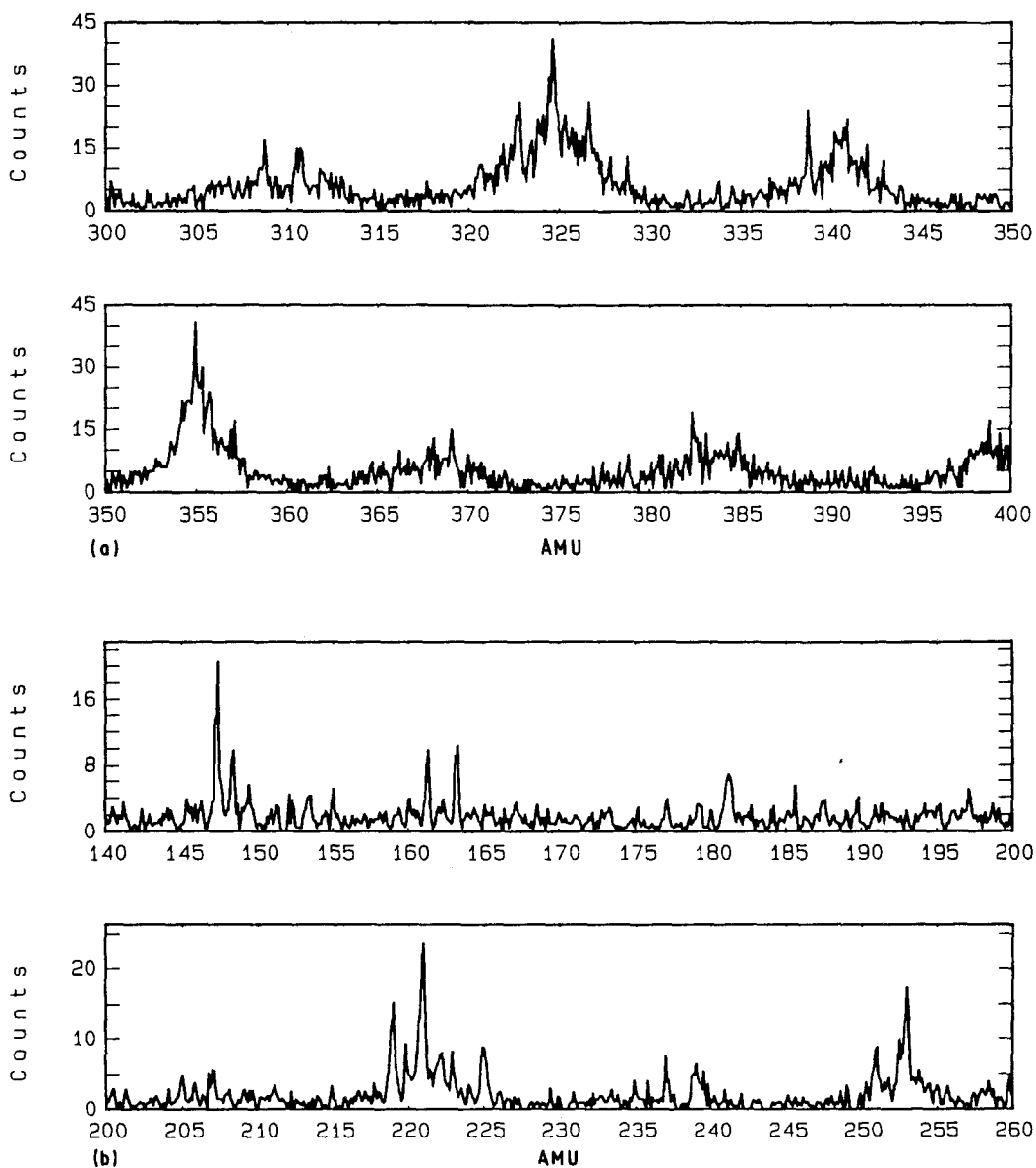


Figure 4 TOF SIMS spectra of (a) the positive ions and (b) the negative ions from the hot-water conditioned as-coated glass slides.

TABLE VII Possible structures for negative ion fragments from the hot-water conditioned as-coated glass slides (The mass number in parentheses refers to the observed fragment in the spectrum.)

AMU	Fragment	AMU	Fragment
163	$\text{CH}_3-\text{Si}(\text{CH}_3)_2-\text{O}-\left[\text{Si}(\text{CH}_3)_2-\text{O}\right]_1$	255 (253)	$\text{HO}-\text{Si}(\text{OH})(\text{NH}_2(\text{CH}_2)_3)-\text{O}-\left[\text{Si}(\text{OH})(\text{NH}_2(\text{CH}_2)_3)-\text{O}\right]_1$
237	$\text{CH}_3-\text{Si}(\text{CH}_3)_2-\text{O}-\left[\text{Si}(\text{CH}_3)_2-\text{O}\right]_2$	221	$\left[\text{Si}(\text{OH})(\text{NH}_2(\text{CH}_2)_3)-\text{O}-\text{Si}(\text{OH})(\text{NH}_2(\text{CH}_2)_3)-\text{O}\right]_0$
149 (147)	$\left[\text{Si}(\text{CH}_3)_2-\text{O}-\text{Si}(\text{CH}_3)_2-\text{O}\right]_0$		

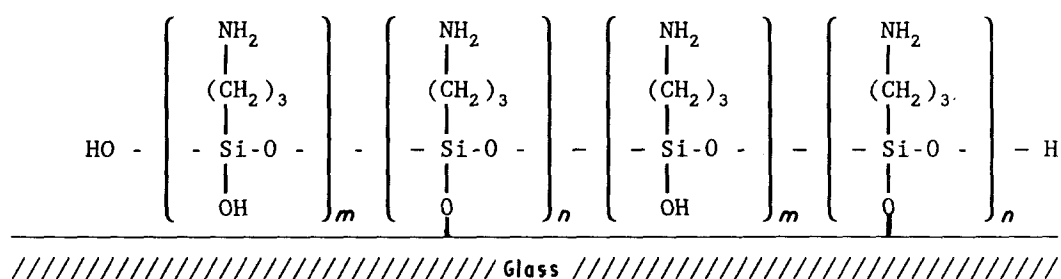


Figure 5 Model of the siloxanol interfacial layer exposed by hot-water extraction.

chemisorbed linearly polymerized or oligomerized layer.

The thickness of this interfacial layer is most likely less than 1 nm because the ion fragments associated with Ca at 40, 56 and 57 AMU, contained in the true glass surface, reappeared after progressive extraction with hot water (Table I). The relative peak intensities compared to the Al peak reached 0.76, totalling about 70% of that for the uncoated glass surface. Similarly, a comparative XPS study of the coated and hot-water extracted plates shows that the latter is dominated by the glass substrate. Therefore, we conclude that

a molecular layer of poly γ -aminopropyl siloxane remains on the immediate glass surface, after hot water extraction for 4 h.

Taking into consideration the Si-O bonds within the glass surface, the difference between a strongly reacted layer and a highly polymerized network is difficult to define. However, if it is assumed that the cyclic structural units arise from partially polymerized siloxane, then it would appear that the interface consists of a strongly bound polymer with a maximum of three adjacent Si-O bonds as typified by the largest secondary ion fragment at 340 AMU. A model of the

interfacial layer is given in Fig. 5 where the presence of siloxane bonds to the glass surface is given.

The siloxane layer also contains partially polymerized structural units, and/or hydrolysed remnants of the three-dimensional layer which would be expected from the random deposition of the hydrolysed APS. Thus the actual structure of the deposit will consist of a polysiloxane chemically bonded to the glass surface at every other silicon atom with occasionally more dense bonding. This can be seen to be consistent with SIMS spectra in Fig. 4 and Table VI. Thus the physisorbed layer consists of low molecular oligomers, overlying a three-dimensionally polymerized siloxane network which grades into a molecular interfacial layer. DiBenedetto and Scola [9] investigated the interaction between APS and S-glass surface using ISS and SIMS with contrasting conclusions. These differences could arise from the differing involvement of the substrate or the sensitivity of the early instruments which did not enable large molecular fragments to be detected. However, these results are consistent with the previous infrared studies [10–12] and demonstrate for the first time the details of the interaction with the glass surface.

5. Conclusions

The presence of components of differing hydrolytic stability in the deposit on an E-glass surface, from an aqueous solution of γ -aminopropyl triethoxysilane, has been confirmed. Using time-of-flight secondary ion mass spectrometry it has been possible to demonstrate a gradation in degree of polymerization from a physisorbed oligomeric component to a three-dimensional network whose apparent network chain length had a degree of polymerization less than 6. At the glass surface, the molecularly thin layer of high hydrolytic stability has a network chain length of degree of polymerization less than 3. The re-emergence of signal from the substrate calcium, after hot-water extraction, demonstrates that this could be less than 1 monolayer thick. The implication is that coverage may not be complete at a 0.05 μm spatial resolution. However, this conclusion is complicated by the incorporation of aluminium from the glass surface and by the copolymerization of the PDMS impurity into the deposit. The dissolution of calcium from the surface also occurs and its presence in the interfacial layer needs further study. However, the results do show clearly that reaction between the surface silanols and the silane deposit has occurred.

Acknowledgements

Financial assistance from SERC and GKN, plc is gratefully acknowledged. We also thank Professor D. Briggs and Dr M. J. Hearn (ICI, plc) for valuable assistance.

References

1. H. A. CLARK and E. P. PLUEDDEMANN, *Mod. Plast.* **40** (1963) 133.
2. E. P. PLUEDDEMANN, "Silane Coupling Agents" (Plenum Press, New York, 1982).
3. D. PAWSON and F. R. JONES, in "Proceedings of the International Conference on Interface Phenomena in Composite Materials", September 1989, Sheffield, edited by F. R. Jones (Butterworth) p. 188.
4. H. R. ANDERSON Jr, F. M. FOWKES and F. H. HIELSCHER, *J. Polym. Sci. Phys.* **14** (1976) 879.
5. R. BAILEY and J. E. CASTLE, *J. Mater. Sci.* **12** (1977) 2049.
6. P. R. MOSES, L. M. WIER, S. C. LENNOK, H. O. FINKEA, J. R. LENHARD and R. W. MURRY, *Anal. Chem.* **50** (1978) 576.
7. J. F. CAIN and E. SACHER, *J. Coll. Interface Sci.* **67** (1978) 539.
8. O. K. JOHANNSON, F. O. STARK, G. E. VOGAL and R. B. FLEISCHMAN, *J. Comp. Mater.* **1** (1967) 278.
9. A. T. DiBENEDETTO and E. SCOLA, *J. Coll. Interface Sci.* **64** (1978) 480.
10. C. H. CHIANG, H. ISHIDA and J. L. KOENIG, *ibid.* **74** (1980) 396.
11. S. R. CULLER, S. NAVIROJ, H. ISHIDA and J. L. KOENIG, *ibid.* **96** (1983) 69.
12. H. ISHIDA, S. NAVIROJ, S. TRIPTYCH, J. J. FITZGERALD and J. L. KOENIG, *J. Polym. Sci. Phys.* **20** (1982) 701.
13. C. H. CHIANG, N. I. LIU and J. L. KOENIG, *J. Coll. Interface Sci.* **86** (1982) 26.
14. T. L. WEEDING, W. S. VEEMAN, L. W. JENNESKENS, H. A. GAUR, H. E. C. SCHUURS and W. G. B. HUYSMANSM, *Macromol.* **22** (1989) 706.
15. J. JANG, H. ISHIDA and E. P. PLUEDDEMANN, in "Interfaces in Polymer, Ceramic and Metal Matrix Composites", edited by H. Ishida (Elsevier, 1988) p. 365.
16. M. E. SCHRADER, I. LERNER and F. J. D'ORLA, *Mod. Plast.* **45** (1967) 195.
17. D. WANG, F. R. JONES and P. DENISON, to be published.
18. D. BRIGGS, *Surf. Interface Anal.* **5** (1983) 113.
19. J. LUB, P. N. T. van VEBEN, D. van LEYEN, B. HAGENHOFF and A. BENNINGHOVEN, *Surf. Interface Anal.* **12** (1988) 53.
20. F. R. JONES (ed.), "Proceedings of the International Conference on Interface Phenomena in Composite Materials", September 1989, Sheffield (Butterworth) p. 25.

Received 7 December 1990
and accepted 15 January 1991